

## 3D Thermo-Electric Modelling of Aluminium Reduction Cells Including Equilibrium Ledge Profile Prediction

Burkhard Sachs<sup>1</sup>, Ingo Eick<sup>2</sup>, Gregor Bellinghausen<sup>3</sup>, Kati Tschöpe<sup>4</sup> and Robert Jørgensen<sup>5</sup>

1. Project Engineer

2. Senior Research Scientist

3. Senior Technology Engineer

Hydro Aluminium Deutschland, Neuss, Germany

4. Project Engineer

5. Principal Engineer

Hydro Aluminium AS, Øvre Årdal, Norway

Corresponding author: burkhard.sachs@hydro.com

### Abstract

Modern aluminium electrolysis cell designs for high amperage, low energy consumption and power flexibility require detailed investigation of spatial heat generation and distribution in the cell as well as of the cooling conditions at the shell outside. To increase the predictive power of thermo-electric modelling for aluminium reduction cells and to streamline the workflow between modelling and detailed design, a parametrized Autodesk Inventor CAD interface was developed and coupled to an ANSYS Workbench thermo-electric simulation. The geometry model includes most details of anode and cathode assemblies as well as of the pot shell. An elaborate iteration scheme is used to calculate equilibrium ledge profiles. This allows for more realistic results that are not compromised by geometrical simplifications or simplified boundary conditions.

**Keywords:** Computer-aided design (CAD), simulation, cell design, heat balance, thermo-electric modeling

### 1. Introduction

Thermal and electric fields in aluminium reduction cells are strongly coupled due to non-linear material properties, extremely high electric currents between 100 and 800 kA and operation temperatures close to 960 °C. Thereby, the thermal stability of an aluminium reduction cell depends on the solidification of electrolyte (ledge) at the inner cell walls, which protects the cell from corrosion and dissolution.

Since the early 1990s partly or full 3D thermo-electrical simulation approaches based on ANSYS® are used in the aluminium industry to predict the heat and voltage balance of cell design upgrades [1, 2]. With improving computer performance, the simulation approaches were extended for transient applications like cell preheating and cathode erosion [3] and coupled to outer convection cooling and inner bath/metal flow simulation approaches [4 - 6]. Detailed analysis of thermo-mechanical and thermo-electro-mechanic effects at anode and cathode blocks and connections followed in the recent years completing the picture [7 - 10].

Today thermo-electrical/mechanical simulations are a common production tool in design and operation improvement which is tightly connected to the local CAD system for realistic geometries. In this paper an integrated and automated approach is presented covering the full span width from CAD design to thermo-electrical/mechanical cell simulation.

The fully automated tool imports the cell geometry from a CAD model into the simulation environment, including the pot shell as well as cathode and anode assemblies. The program

continues by defining model settings, boundary conditions and standard results visualisation and initiates the simulation. The solver routines encompass an elaborate iteration scheme with alternating thermal-electric and structural-mechanical solutions, supported by mesh non-linear adaptivity, to finally obtain a consistent thermal-electric solution at ledge phase equilibrium.

This paper is structured as follows: Section 2 explains the simulation approach in general, such as interlinks to CAD software and the advantages of realistic and detailed model geometries. To underline this, the role of welding seams in the pot shell of the Neuss smelter is given as an example. The ledge calculation scheme is discussed as well. Section 3 gives an impression on typical calculation results. Finally, a conclusion and an outlook are given in Section 4.

## 2. Thermo-electric simulation method

The primary purpose of a cell design tool is the calculation of the heat balance, which underlies, for pots in thermal balance, the following equation:

$$Q_{inn} + Q_{out} = 0 \quad (1)$$

where  $Q_{inn}$  describes total inner heat input to the cell, and  $Q_{out}$  denotes the heat losses to outside over the potshell, superstructure, hooding, and so on.

It should be noted that the main heat source in the cell, the Joule heating, is a locally varying quantity. Thus, a purely thermal heat conduction problem with averaged Joule heating contributions would not adequately describe the spatial heat distribution within the cell. Instead, a coupled thermal and electric approach has to be chosen based on temperature-dependent individual thermal and electrical conductivities, which involves the local currents within the pot. The following coupled equations constitute the stationary heat conduction problem including Joule heating terms:

$$-\nabla(\lambda\nabla T) = \sigma(\nabla V)^2 \quad (2)$$

$$\nabla(\sigma\nabla V) = 0 \quad (3)$$

Here,  $\lambda$  and  $\sigma$  denote temperature-dependent thermal and electrical conductivities, respectively, while  $T = T(x, y, z)$  and  $V = V(x, y, z)$  are the solution functions of the temperature and electric potential defined for space variables  $x, y, z$ . For further mathematical insight on coupled-field equations solved in a FE thermo-electric analysis in ANSYS, see, e.g., Antonova and Looman [11].

### 2.1. Integrated Modelling Approach

To enable a wide functionality based on a realistic cell geometry including full shell, cathode and anode details, an integrated modelling approach was chosen. In this way, the geometry can be automatically generated by the CAD system, Autodesk Inventor, based on a parameter list and controlled by a graphical user interface (GUI). After setting up the geometry and applying the material properties, the necessary boundary conditions are selected in the GUI and the simulation is automatically initiated within ANSYS Workbench (see Figure 1). Upon finishing the calculations, result tables with design information and a selection of result plots are generated.

Several benefits accompany this approach. The high level of geometry parametrization allows generating detailed CAD models and interlinking these with a state-of-the-art simulation environment. Thereby, manual user work is solely done within the GUI, thus, without the

requirement of being an expert in both Inventor and ANSYS. Moreover, the full automation reduces the risk of errors, both within the CAD model, but also within the simulation set-up. Typical errors during manual handling would be collisions and gaps between assembly components, incorrect material assignments or missing boundary conditions.

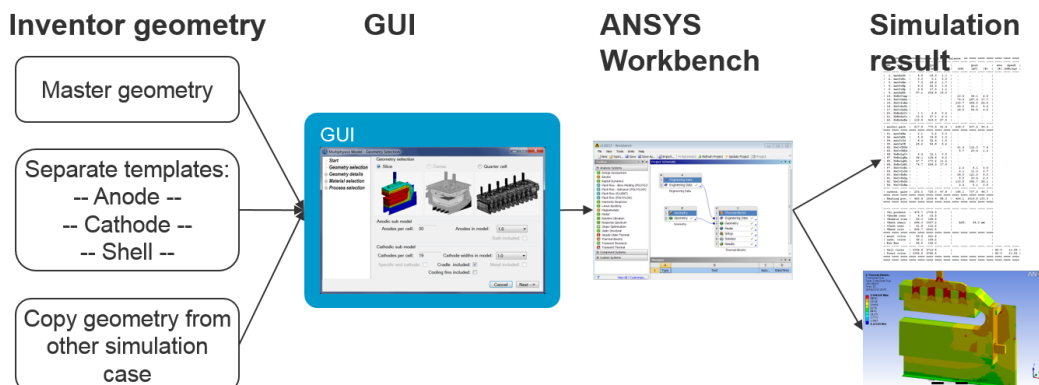


**Figure 1. Interlink of CAD with simulation environment controlled via a home-made GUI.**

## 2.2. Realistic Geometry and Material Properties

Beside accurate calculation of the current distributions within the anode cathode assemblies, another good reason for detailed CAD-based geometries is the pot shell. Here, details appearing subtle at first sight, can play a crucial role for the heat distribution within the pot. A good example is the welding seam of the pot cradle in the Neuss Rheinwerk smelter, see Figure 2.

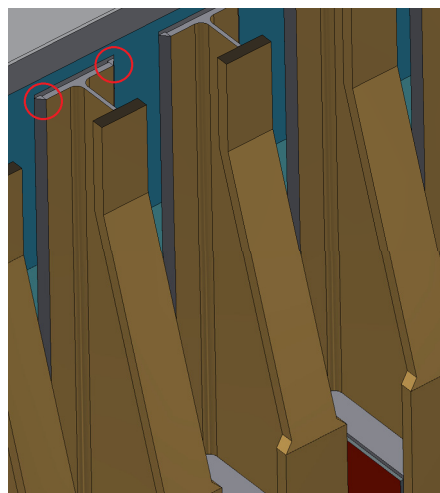


**Figure 2. Example of a double flange side cradle with welding seams (in red circles) included.**

This cradle construction involves two flanges, with one flange being welded to the pot shell. Heat flux measurements show that this special cradle type pulls a considerable amount of heat out of the cell, contributing by roughly 40 % to the total outer heat loss. Since the thermal bridge between the cradle and the pot shell is rather the welding seam than the flange itself, it is obvious that a model assuming a large thermal contact area between the flange and the shell would overestimate the cooling effect of the cradles. Here, consideration of welding seams in combination with a suppression of direct thermal contact between the flange and the shell allows for satisfying agreement between measurements and model results.

### **2.3. Automated Simulation Build-up and Execution**

Once the CAD model is generated, the transfer of the geometry to ANSYS is initiated. Here, the pure geometrical information is not sufficient, because each body has to be linked to a material property. Furthermore, boundary conditions need to be applied to individual body faces. This can be achieved by the ANSYS plug-in within Inventor. The model import, including definition of material tables, material and boundary conditions assignments is then done in Workbench via combined Python and JScript scripts. All geometry, material and simulation parameters are processed via XML files. Once the model setup is prepared, the ANSYS solver is called and solver routines are run, written in the ANSYS parametric design language (APDL). The main tasks of the APDL routines are the ledge equilibrium calculation (Section 2.4.2) and the generation of model output results (Section 3).

### **2.4. Thermal Ledge Equilibrium by Adaptive Meshing Approach**

#### **2.4.1. Inner Boundary Conditions**

In an aluminium reduction cell, the Joule heating generated by current-conducting solids (mainly steel, carbon, and aluminium) as well as by molten liquids (electrolyte, aluminium) constitutes the inner power of heating. To reduce computational efforts, molten liquids are not represented as physical bodies in our FE model. Instead, these are taken into account effectively via inner convection boundary conditions.

In reality, the inner heat conditions within a cell are not simple to assess and are highly local. Flow-driven heat transfer between the ledge and the bath originates from gas bubble formation under the anodes, but also from metal flow, which is itself driven by large Lorentz forces.

At the interface of ledge and metal, similar heat transfer coefficients as in the bath are assumed despite a very high thermal conductivity of aluminium compared to cryolite. According to latest research, this may be justified by the existence of a bath film between the ledge and the liquid metal [12].

#### **2.4.2. Calculation of Ledge Profile**

Having established the set of inner boundary conditions, the challenge remains in predicting the equilibrium ledge profile. Since the ledge is a strong thermal insulator, the heat distribution in the side and end lining is highly sensitive to the extent of the ledge. Moreover, a strong thermo-electric interplay is given at the cathode surface by the formation of bottom ledge, which controls the surface current density on the cathode block and thereby the cathodic voltage drop (CVD). The accuracy of thermal and voltage balances thus strongly relies on a precise prediction of the equilibrium ledge.

For this purpose, our FE model follows an iterative ledge optimization scheme. An equilibrium solution is only achieved if the surface temperatures on the ledge front match the phase transition temperature (i.e., the liquidus temperature of the electrolyte). Technically, this means that all ledge front nodes in the FE model need to be individually evaluated in temperature, and the phase boundary has then to be relocated according to the difference to the phase transition temperature. These work steps are repeated until the final equilibrium solution is obtained. For a typical quarter cell model with 300 000 to 600 000 elements, one iteration takes between 5 and 30 minutes on a modern multi-core desktop computer, depending on individual performance parameters (processor, memory, hard drive).

### 2.4.3. Adaptive Remeshing of the Ledge

During the ledge calculation process, the ledge can be strongly deformed, depending on the boundary conditions, the initial and the final equilibrium ledge shape. Large body deformation is problematic in FE models. As soon as the mesh gets degraded in quality, this induces significant numerical errors. This problem can be cured by a remeshing of the deformed ledge. ANSYS offers a convenient condition for the remeshing of highly deformed tetrahedral elements, which is given by the volume-based skewness,

$$S_i = \frac{V_0 - V_i}{V_0} \quad (4)$$

where  $V_0$  is the volume of a regular tetrahedron circumscribed by the same sphere as the deformed element  $i$  with volume  $V_i$ . For linear tetrahedral elements, the skewness is always between 0 (regular tetrahedron) and 1 (flat tetrahedron). Those elements with a skewness higher than the defined threshold (typically  $\sim 0.9$ ) are taken as seed elements for a certain element region to be remeshed (cf. Figure 3). In this way, element skewness can be brought down or at least kept at an acceptable level.

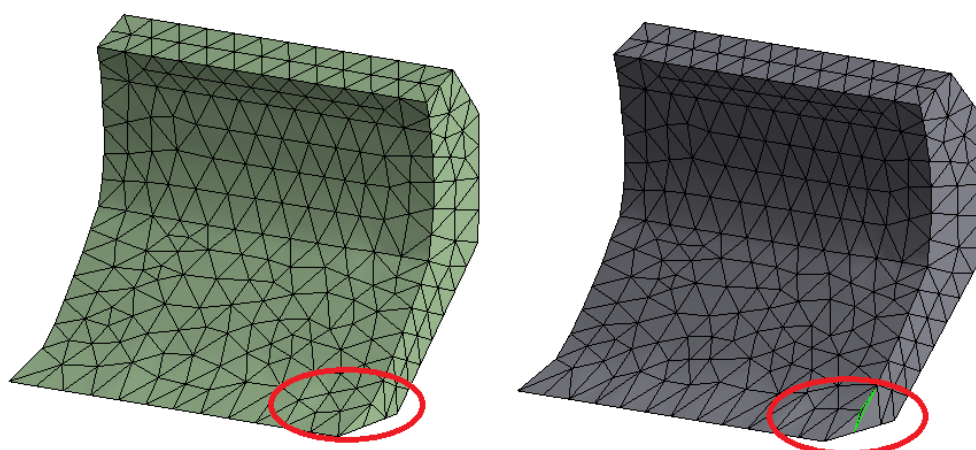


**Figure 3. Slice model: example of a remeshed ledge (left) vs. a ledge without remeshing (right). During ledge calculation, elements can be highly distorted (right side, red circle: an extremely flat tetrahedron is marked by green lines), while good element quality is maintained by remeshing (left side, red circle: no flat tetrahedra).**

## 3. Modelling Results

Having obtained a converged calculation, the task remains to evaluate the results, which are at first solely the temperature and electric potential values for individual nodes within the FE model. Typical results (e.g., heat fluxes, current densities and so on) may then be easily derived and visualized using ANSYS result objects. Examples are shown in Figure 4.

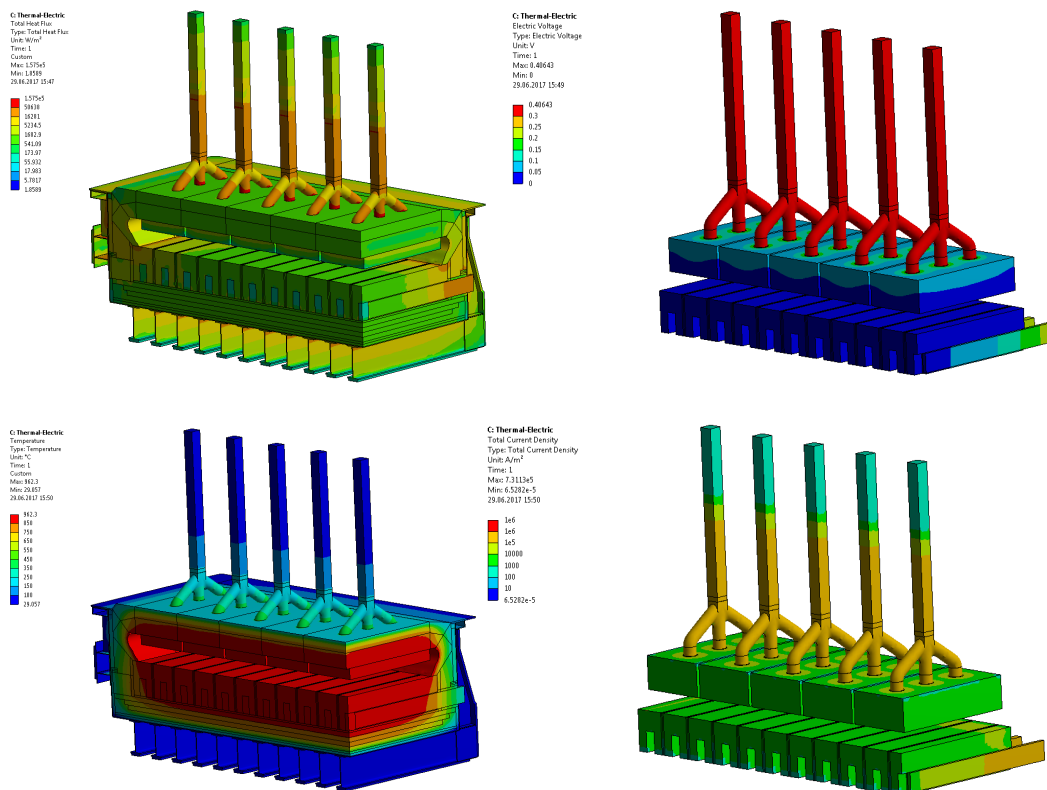


**Figure 4: Result output examples for a quarter cell model. Top left: heat flux. Top right: electric potential. Bottom left: temperatures. Bottom right: current densities.**

Additionally, a thorough post-processing of the solution is carried out to condense important results into output tables. Most important results are aggregated into voltage and heat balance tables. Moreover, individual material properties and typical design-related results, such as critical temperatures in the insulation bricks, can be obtained from further large output tables.

#### 4. Conclusions and Outlook

The presented simulation approach combines state-of-the-art FEM thermo-electric calculations with detailed geometries based on CAD. This allows predicting accurate heat and voltage balances during design of aluminium reduction cells. A special focus was placed on the equilibrium ledge calculation, which crucially determines the cell properties. Here, further functionality will be added in the future, such as burn-off anode shape and phase boundaries within the anode cover material.

Moreover, the developed interface between CAD-based model generation and FE simulations is a versatile and flexible approach. It will be extended in the future for thermo-mechanical applications, e.g., for predictions of crack formation in cell lining and evaluation of pot shell stability. Beyond that, transient thermo-mechanical approaches would be of further interest, e.g., to optimize cell start-up procedures. Finally, fully coupled thermo-electrical-mechanical simulations may be developed to cover delicate material contact problems, such as carbon-steel contact during cell operation.

#### 5. Acknowledgement

We are grateful to Rheinwerk smelter Neuss for publishing the given figures and results.

## 6. References

1. Marc Dupuis, Imad Tabsh, Thermo-electric analysis of the grande-baie aluminum reduction cell, *Light Metals* 1994, 339-342.
2. Detlef Vogelsang et al., From 110 to 175 kA, Retrofit of VAW Rheinwerk, Part I: Modernisation Concept, *Light Metals* 1997, 233-238.
3. Marc Dupuis, Development of a 3D transient thermo-electric cathode panel erosion model of an aluminum reduction cell, *CIM* 2000, 169-178.
4. Detlef Vogelsang, Ingo Eick, Dimensioning of cooling fins for high-amperage reduction cells, *Light Metals* 1999, 339.
5. M. Dupuis, V. Bojarevics, J. Freibergs, Demonstration thermo-electric and MHD mathematical models of a 500 kA Al electrolysis cell, *CIM* 2003, 3-20
6. Gennady V. Arkhipov, Alexander V. Rozin, The aluminum reduction cell closed system of 3D mathematical models, *Light Metals* 2005, 589-592.
7. Marc Dupuis, Development and application of an ansys based thermo-electro-mechanical collector bar slot design tool, *Light Metals* 2011, 519-524.
8. D.R. Gunasegaram, D. Molenaar, A fully coupled thermal-electrical-mechanical transient fea model for a 3D anode assembly, *Light Metals* 2013, 1341-1346.
9. Mathieu Gagnon et al., Optimization of the cathode collector bar with a copper insert using finite element method, *Light Metals* 2013, 621-626.
10. Dag Herman Andersen and Hogne Linga, Evaluating the crack resistance of carbon anodes: Implementation of a measurement system for tensile strength and fracture toughness, *Light Metals* 2015, 1123-1128.
11. E. E. Antonova and D. C. Looman, Finite elements for thermoelectric device analysis in ANSYS, *ICT 2005. 24th International Conference on Thermoelectrics*, 2005, 215-218.
12. Asbjørn Solheim, Nils-Håvard Giskeødegård, and Nancy J. Holt, Sideledge facing metal in aluminium electrolysis cells: Freezing and melting in the presence of a bath film", *Light Metals* 2016, 333-338.

